$Os(phen)_2dppz^{2+}$ in Photoinduced DNA-Mediated Electron Transfer Reactions

R. Erik Holmlin, Eric D. A. Stemp, and Jacqueline K. Barton*

Contribution from the Division of Chemistry and Chemical Engineering and Beckman Institute, California Institute of Technology, Pasadena, California 91125

Received November 27, 1995[⊗]

Abstract: The photoinduced electron transfer chemistry between $Os(phen)_2dppz^{2+}$ and $Rh(phi)_2bpy^{3+}$ bound to DNA has been characterized. $Os(phen)_2dppz^{2+}$ serves as an isostructural analogue for $Ru(phen)_2dppz^{2+}$ with a red-shifted emission spectrum, access to a 3+ oxidation state which is stabilized by ~500 mV relative to the ruthenium complex, and excited-state lifetimes below 10 ns in the presence of DNA. Emission from Δ-$Os(phen)_2dppz^{2+}$ bound to calf thymus DNA is efficiently quenched by Δ-$Rh(phi)_2bpy^{3+}$, and a lower limit for the quenching constant is set at 7×10^9 s^{-1}. The quenching profile over a range of quencher concentrations is found to be remarkably similar to that of the ruthenium analogue, despite an increase of ~200 mV in ΔG for the photoinduced, forward electron transfer reaction. Such an observation may indicate the importance of the HOMO energy in the donor excited state, which is similar for both donors. Owing to the lack of spectral overlap between $Os(phen)_2dppz^{2+}$ emission and $Rh(phi)_2bpy^{3+}$ absorption, energy transfer does not contribute to the observed quenching, and therefore, on the basis of the similarity in quenching profiles for the osmium and ruthenium donors, we can also rule out energy transfer in the photoinduced quenching of intercalated $Ru(phen)_2dppz^{2+}$ by $Rh(phi)_2bpy^{3+}$. Moreover, diffusional processes are found not to contribute to quenching, since the faster intrinsic excited state of the osmium complex compared to ruthenium does not lead to a reduction in quenching efficiency. Transient absorption measurements on the microsecond time scale furthermore reveal a transient signal for this electron transfer process, and this transient intermediate has been assigned to the oxidized donor (Os(III)) on the basis of full spectral characterization and comparison to chemical oxidation of Os(II).

Introduction

Increasingly, theoretical[1−3] and experimental[4−10] studies have been directed toward elucidating the role of the DNA double helix in mediating electron transfer between donors and acceptors bound to the polymer. The DNA double helix may be described as two intertwined polymers containing a linear array of π-stacked, aromatic, heterocyclic bases within a polyanionic sugar−phosphate backbone. Independent of its biological function, such a polymeric assembly provides an ideal medium through which a detailed study of electron transfer mediated by a π-stack may be accomplished in solution. Recent experiments in our laboratories have focused on electron transfer reactions between transition-metal complexes which bind tightly to DNA by intercalation (metallointercalators).[10] Through their intercalative stacking, these metal complexes provide a direct means to probe the DNA π-stack. Previously, we reported the photoinduced quenching of intercalated $Ru(phen)_2dppz^{2+}$ (dppz = dipyrido[3,2-*a*:2′,3′-*c*]phenazine) by $Rh(phi)_2phen^{3+}$ (phi = 9,10-phenanthrenequinone diimine) in DNA.[10a] Both $Ru(phen)_2dppz^{2+}$ and $Rh(phi)_2phen^{3+}$ bind tightly to DNA ($K_D \sim 10^{-7}$ M) by intercalation from the major groove.[11,12] Additionally, $Ru(phen)_2dppz^{2+}$ serves as a molecular light switch for DNA.[11] Although the complex luminesces in organic solvents, emission from the metal-to-ligand charge-transfer (MLCT) excited state is quenched in aqueous solution owing to interaction between the solvent hydrogens and the phenazine nitrogens of the dppz ligand.[13] Upon binding to DNA by preferential intercalation of the dppz ligand, these phenazine nitrogens are protected from water, and luminescence returns. Analogous light switch behavior has recently been described for a rhenium(I) complex containing the dppz ligand.[14]

DNA-mediated electron transfer quenching of $Ru(phen)_2dppz^{2+}$ by rhodium intercalators appears to be fast[10a,15] and to occur over some distance.[10b] At low loadings of $Ru(phen)_2$-

* Author to whom correspondence should be addressed.

⊗ Abstract published in *Advance ACS Abstracts,* May 15, 1996.

(1) Felts, A. K.; Pollard, W. T.; Friesner, R. A. *J. Phys. Chem.* **1995**, *99*, 2929.

(2) (a) Kemp, M.; Mujica, V.; Ratner, M. A. *J. Chem. Phys.* **1994**, *101*, 5172. (b) Mujica, V.; Kemp, M.; Ratner, M. A. *J. Chem. Phys.* **1994**, *101*, 6849. (c) Mujica, V.; Kemp, M.; Ratner, M. A. *J. Chem. Phys.* **1994**, *101*, 6856.

(3) Risser, S. M.; Beratan, D. N.; Meade, T. J. *J. Am. Chem. Soc.* **1993**, *115*, 2508.

(4) Baguley, B. C.; LeBret, M. *Biochemistry* **1984**, *23*, 937.

(5) Fromherz, P.; Rieger, B. *J. Am. Chem. Soc.* **1986**, *108*, 5361.

(6) (a) Brun, A. M.; Harriman, A. *J. Am. Chem. Soc.* **1992**, *114*, 3656. (b) Brun, A. M.; Harriman, A. *J. Am. Chem. Soc.* **1994**, *116*, 10383.

(7) Meade, T. J.; Kayyem, J. F. *Angew. Chem., Int. Ed. Engl.* **1995**, *34*, 352.

(8) Johnston, D. H.; Glasgow, K. C.; Thorp, H. H. *J. Am. Chem. Soc.* **1995**, *117*, 8933.

(9) (a) Barton, J. K.; Kumar, C. V.; Turro, N. J. *J. Am. Chem. Soc.* **1986**, *108*, 6391. (b) Purugganan, M. D.; Kumar, C. V.; Turro, N. J.; Barton, J. K. *Science* **1988**, *241*, 1645.

(10) (a) Murphy, C. J.; Arkin, M. R.; Ghatlia, N. D.; Bossmann, S.; Turro, N. J.; Barton, J. K. *Proc. Natl. Acad. Sci. U.S.A.,* **1994**, *91*, 5315. (b) Murphy, C. J.; Arkin, M. R.; Jenkins, Y.; Ghatlia, N. D.; Bossmann, S.; Turro, N. J.; Barton, J. K. *Science* **1993**, *262*, 1025.

(11) (a) Friedman, A. E.; Chambron, J.-C.; Sauvage, J.-P.; Turro, N. J.; Barton, J. K. *J. Am. Chem. Soc.* **1990**, *112*, 4960. (b) Jenkins, Y.; Friedman, A. E.; Turro, N. J.; Barton, J. K. *Biochemistry* **1992**, *31*, 10809. (c) Hartshorn, M.; Barton, J. K. *J. Am. Chem. Soc.* **1992**, *114*, 5919. (d) Dupureur, C. M.; Barton, J. K. *J. Am. Chem. Soc.* **1994**, *116*, 10286.

(12) (a) Sitlani, A.; Long, E. C.; Pyle, A. M.; Barton, J. K. *J. Am. Chem. Soc.* **1992**, *114*, 2303. (b) David, S. S.; Barton, J. K. *J. Am. Chem. Soc.* **1993**, *115*, 2984. (c) Uchida, K.; Pyle, A. M.; Morii, T.; Barton, J. K. *Nucleic Acids Res.* **1989**, *17*, 10259.

(13) Turro, C.; Bossman, S. H.; Jenkins, Y.; Barton, J. K.; Turro, N. J. *J. Am. Chem. Soc.* **1995**, *117*, 9026.

(14) Stoeffler, H. D.; Thornton, N. B.; Temkin, S. K.; Schanze, K. S. *J. Am. Chem. Soc.* **1995**, *117*, 7119.

(15) Arkin, M. R.; Stemp, E. D. A.; Holmlin, R. E.; Barton, J. K.; Hormann, A.; Olson, E. J. C.; Barbara, P. A. *Science,* in press.

S0002-7863(95)03941-2 CCC: $12.00

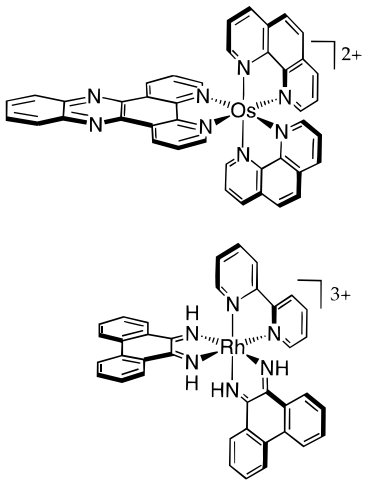

Figure 1. Schematic illustration of Δ-Os(phen)$_2$dppz^{2+} (top) and Δ-Rh(phi)$_2$bpy^{3+} (bottom).

dppz^{2+} and Rh(phi)$_2$phen^{3+} on the helix, where the average donor−acceptor separation is large, the photoinduced electron transfer quenching and subsequent recombination[15] were found to proceed on a subnanosecond time scale. In contrast, the groove−bound acceptor Ru(NH$_3$)$_6^{3+}$ quenches the DNA-bound Ru(phen)$_2$dppz^{2+} more slowly through a collisional mechanism.[10a] Additionally, in an assembly with the ruthenium donor and the rhodium acceptor tethered by a flexible linker to opposite ends of a 15-mer duplex, where the reactants are intercalated but separated by ∼40 Å, the ruthenium steady-state emission is fully quenched.[10b] A lower limit for the quenching rate constant was set at 3×10^9 s^{-1} over this large molecular distance. On the basis of energetic considerations, electron transfer was considered the most likely mechanism responsible for this remarkable long-range quenching. Using the donor and acceptor analogues Ru(DMP)$_2$dppz^{2+} (DMP = 4,7-dimethylphenanthroline) and Rh(phi)$_2$bpy^{3+}, respectively, a long-lived intermediate corresponding to the oxidized donor was recently observed by transient absorption spectroscopy, providing the first direct evidence for DNA-mediated electron transfer between metallointercalators.[16]

Many issues concerning the nature of the observed DNA-mediated quenching require further consideration. For example, owing to a small but nonzero overlap between donor (Ru(II)) emission and acceptor (Rh(III)) absorption, an energy transfer mechanism may also contribute to the quenching. Additionally, we would like to address the effect of the donor energetics and intrinsic excited-state lifetime on the efficiency of this quenching with DNA as the bridge.

Hence, in order to expand the scope of DNA-mediated electron transfer reactions between metallointercalators and to begin to address these issues, we have now applied dppz complexes of osmium as electron donors. Indeed, Os(phen)$_2$dppz^{2+} (Figure 1) also serves as a molecular light switch for DNA, providing a red-emitting DNA probe with excited-state lifetimes faster than 10 ns.[17] Substitution of osmium should not alter the DNA binding properties of the metal complex but, rather, provide an isostructural analogue for Ru(phen)$_2$dppz^{2+} with distinct photophysical and electrochemical properties.[18] Importantly, as shown in Figure 2, the emission spectrum of intercalated Os(phen)$_2$dppz^{2+} is red-shifted by ∼120 nm compared to its ruthenium counterpart. This long-wavelength emission does not overlap the rhodium absorption.

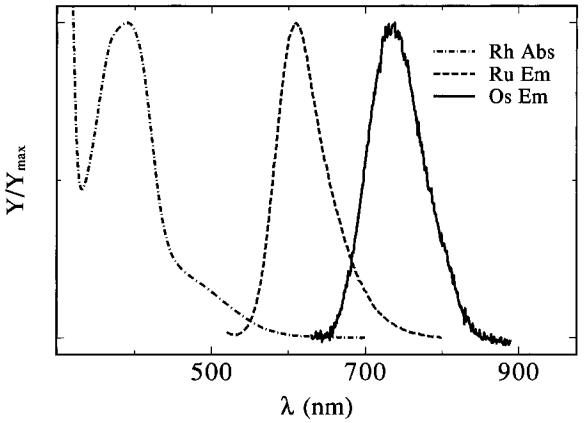

Figure 2. Visible absorption spectrum of Rh(phi)$_2$bpy^{3+} bound to DNA compared to the emission spectra of intercalated Ru(phen)$_2$dppz^{2+} (λ_{max} = 617 nm) and Os(phen)$_2$dppz^{2+} (λ_{max} = 738 nm). The red emission from the osmium complex bound to DNA does not overlap the rhodium absorption.

Thus, energy transfer[19] is not a consideration when studying the quenching of Os(phen)$_2$dppz^{2+} by rhodium intercalators, and the comparison between ruthenium and osmium quenching profiles allows for the identification of any energy transfer quenching in the ruthenium example. Additionally, the fast intrinsic excited-state lifetimes of DNA-bound osmium compared to Ru(phen)$_2$dppz^{2+} allow one to evaluate the contribution of dynamic collisional processes to the quenching. In this report, we therefore describe the DNA binding and electrochemical properties of Os(phen)$_2$dppz^{2+} as well as the DNA-mediated electron transfer chemistry between intercalated Os(phen)$_2$dppz^{2+} and Rh(phi)$_2$bpy^{3+} (Figure 1) bound to DNA.

Experimental Section

Materials. [Os(phen)$_2$dppz](PF$_6$)$_2$ was prepared as described previously[17] and exchanged to the dichloride salt by anion-exchange chromatography (1:1 acetonitrile/water eluent) on Sephadex QAE-25 (Aldrich). [Rh(phi)$_2$bpy]Cl$_3$ was also prepared as reported.[20] Trace impurities were rigorously excluded by high-pressure liquid chromatography. Resolution of the racemic mixtures was achieved using standard methodology.[11,12b,21] Resolution of Os(phen)$_2$dppz^{2+} proceeded with base line separation of the two enantiomers on the anion-exchange column, and absolute configuration was assigned by comparison to Δ-Ru(phen)$_2$dppz^{2+}. For Δ-Os(phen)$_2$dppz^{2+}, $\Delta\epsilon$(270 nm) = −355 M^{-1} cm^{-1}. Sonicated and phenol-extracted calf thymus DNA (Sigma) was exchanged into standard buffer (5 mM tris, 50 mM NaCl, pH 8.5) by ultrafiltration (Amicon). [Ru(NH$_3$)$_6$]Cl$_3$ was purchased from Aldrich and used as received.

Instrumentation. Time-correlated single photon counting (TCSPC) and time-resolved measurements on the nanosecond time scale were carried out using the facilities in the Beckman Institute Laser Resource Center (BILRC) described previously.[17,22] TCSPC data sets were typically counted until 5,000−10000 counts accumulated in the highest channel. Excitation for transient absorption and nanosecond time scale emission experiments was provided by an excimer-pumped dye laser (1−5 mJ/10 ns pulse) containing either Coumarin 480 (480 nm;

(16) Stemp, E. D. A; Arkin, M. R.; Barton, J. K. *J. Am. Chem. Soc.* **1995**, *117*, 2375.
(17) Holmlin, R. E.; Barton, J. K. *Inorg. Chem.* **1995**, *34*, 7.
(18) (a) Creutz, C.; Chou, M.; Netzel, T. L.; Okumura, M.; Sutin, N. *J. Am. Chem. Soc.* **1980**, *102*, 1309. (b) Kober, E. M.; Sullivan, B. P.; Dressick, W. J.; Caspar, J. V.; Meyer, T. J. *J. Am. Chem. Soc.* **1980**, *102*, 7385. (c) Creutz, C. Sutin, N. *Inorg. Chem.* **1976**, *15*, 496. (d) Nazeeruddin, M. K.; Zakeeruddin, S. M.; Kalyanasundaram, K. *J. Phys. Chem.* **1993**, *97*, 9607. (e) Decola, L.; Balzani, V.; Barigelletti, F.; Flamigni, L.; Belser, P.; Von Zelewsky, A. *Inorg. Chem.* **1993**, *32*, 5228.
(19) Turro, N. J. *Modern Molecular Photochemistry*, Benjamin Cummings: Menlo Park, CA, 1978.
(20) Pyle, A. M.; Chiang, M. Y.; Barton, J. K. *Inorg. Chem.* **1990**, *29*, 4487.
(21) Yoshikawa, Y.; Yamasaki, K. *Coord. Chem. Rev.* **1979**, *28*, 205.
(22) Friedman, A. E.; Kumar, C. V.; Turro, N. J.; Barton, J. K. *Nucleic Acids Res.* **1991**, *19*, 2595.

Exciton) or Rhodamine 6G (580 nm; Exciton), or by a frequency-doubled Nd:YAG laser which provided 15−25 mJ/8 ns pulse at 532 nm. A pulsed 75 W Xe-arc lamp (Photon Technology International) served as the probe source for transient absorption experiments. Individual data sets were typically the average of 400−2500 shots. Data fitting was accomplished by the least-squares method of Marquardt using both in-house (BILRC) and commercial (Axum, Trimetrix) software. Emission spectra were recorded on an SLM 8000 spectrofluorimeter and standardized to $Ru(bpy)_3^{2+}$ (emission maximium = 607 nm).[23] Ultraviolet−visible (UV−vis) absorption spectra were recorded on a Cary 2200 spectrophotometer.

Methods. Photophysical studies were carried out at ambient temperature in aerated solutions. Emission quenching was quantitated by integration of the response-limited excited-state decays on the nanosecond time scale or by steady-state measurements; both methods gave equivalent results. Plots of the fraction of intensity quenched (fraction quenched = $1 - I/I_0$) versus quencher concentration are reported here, given the substantial quenching evident and the low signal to noise observed at high quencher concentrations which are overemphasized in plots of I_0/I. Importantly, plots of I_0/I for these data curve upward with increasing quencher, indicating that the Stern−Volmer analysis is not appropriate. Quenching titrations were typically carried out with the addition of aliquots of concentrated acceptor solution to samples containing DNA and donor. Identical results were obtained if separate samples were prepared for each quencher concentration.

Absorbance difference spectra of long-lived intermediates were generated as follows. Individual data traces at a given wavelength were fit to an exponential function at times > 1 μs (20 × bandwidth), and the absorbance change was obtained by extrapolation of the fit back to time zero, thus eliminating interference from the short-lived $Os(phen)_2dppz^{2+}$ excited state. The kinetics of the long-lived transients were independent of wavelength, indicating that a single reaction was being monitored.

Oxidation of $Os(phen)_2dppz^{2+}$ to $Os(phen)_2dppz^{3+}$ was achieved by addition of 10 μL aliquots of a freshly prepared aqueous solution of $(NH_4)_2[Ce(NO_3)_6]$ (10 mg/mL) and monitored by UV−vis spectrophotometry.

Electrochemical Measurements. Reduction potentials were determined by cyclic voltammetry (CV) using instrumentation described previously.[10a] Complexes were dissolved in dry DMF (Fluka; stored over molecular sieves) containing 0.1 M tetrabutylammonium hexafluorophosphate as supporting electrolyte. Electrochemical windows ranging from 0.2 to 1.6 V *vs* NHE for oxidation, and from 0.2 to −1.55 V *vs* NHE for reduction, were scanned at a rate of 0.1 V/s.

Results

DNA Binding Properties. Visible absorption spectroscopy as well as time-resolved luminescence measurements have been used to characterize the intercalative binding of the $Os(phen)_2dppz^{2+}$ to double-helical DNA. Figure 3 shows the effect of increasing DNA concentration on the $Os(phen)_2dppz^{2+}$ visible absorption spectrum, consisting of an intraligand (IL) $\pi-\pi^*$ transition centered on the phenazine portion of the dppz ligand [λ_{max} = 372 nm: $\epsilon = 1.3 \times 10^4\ M^{-1}\ cm^{-1}$], and ^{1}MLCT states ($\lambda_{max}$ = 430, 472 nm). As the DNA concentration is increased, pronounced hypochromism is observed in the IL band as well as in the MLCT transitions, with an isosbestic point at 505 nm. The percent hypochromism at 372 nm, plotted against the nucleotide:osmium ratio ($R_{nuc:Os}$) in Figure 3 (inset), increases linearly until reaching saturation with a 38% decrease in absorbance at $R_{nuc:Os} \simeq 5$. The IL band is also red shifted ~7 nm over the course of the titration. Such a hypochromic effect is consistent with the preferential intercalative stacking of the dppz ligand and has also been observed for $Ru(phen)_2dppz^{2+}$ over the same concentration range.[11,24]

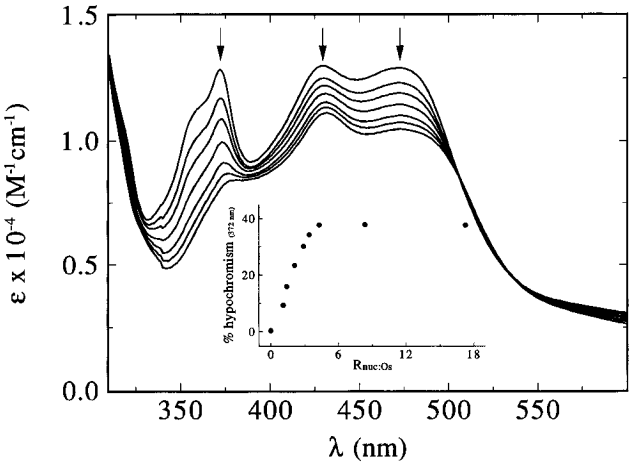

Figure 3. Visible absorption spectra of racemic $Os(phen)_2dppz^{2+}$ in the presence of increasing DNA concentrations. DNA-nucleotide to osmium ratios ($R_{nuc:Os}$) shown are as follows: 0, 1.1, 1.4, 2.1, 2.9, 3.4, 4.3. The metal concentration was held constant, and any absorbance contribution by the DNA was subtracted. Conditions: 35 μM Os, 5 mM Tris, 50 mM NaCl, pH 8.5. Inset: Plot of percent hypochromism [$((A_{R=0} - A_{R=x})/A_{R=0}) \times 100$)] at 372 nm versus $R_{nuc:Os}$. Shown are $R_{nuc:Os}$ = 0, 1.1, 1.4, 2.1, 2.9 3.4, 4.3, 8.3, 17.2.

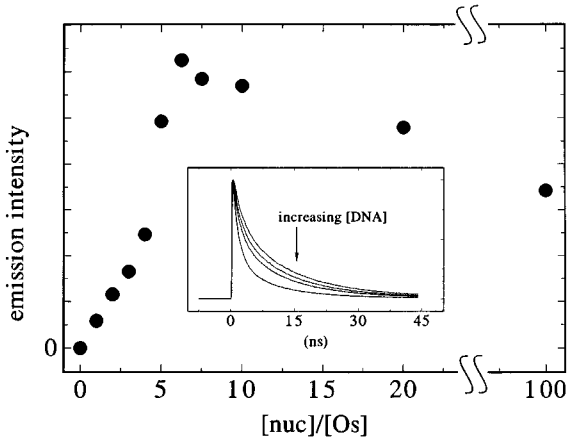

Figure 4. Plot of Δ-$Os(phen)_2dppz^{2+}$ emission intensity as a function of the DNA-nucleotide to osmium ratio ($R_{nuc:Os}$). Shown are $R_{nuc:Os}$ = 0, 1, 2, 3, 4, 5, 6.25, 7.5, 10, 20, 100. Conditions: 20 μM Os, 5 mM Tris, 50 mM NaCl, pH 8.5. Inset: Plot of emission counts versus time for Δ-$Os(phen)_2dppz^{2+}$ bound to DNA at $R_{nuc:Os}$ = 5, 10, 20, 100 as measured by TCSPC. Conditions: 50 μM Os, 5 mM Tris, 50 mM NaCl, pH 8.5. λ_{exc} = 590 nm; λ_{obs} = 775 nm.

The luminescence intensity for Δ-$Os(phen)_2dppz^{2+}$ is plotted as a function of $R_{nuc:Os}$ in Figure 4. Owing to the molecular light switch characteristic of $Os(phen)_2dppz^{2+}$,[17] no emission is detected for the complex in aqueous solution in the absence of DNA. As DNA is titrated into the solution, luminescence is observed. The emission yield increases smoothly with increasing DNA approaching $R_{nuc:Os} \simeq 5$, consistent with the absorption titration. However, increasing the DNA concentration beyond $R_{nuc:Os}$ = 5 produces a significant increase in the emission yield which maximizes at $R_{nuc:Os}$ = 6.25. Interestingly, with further addition of DNA, the emission yield actually decreases slightly.

To examine more closely the DNA concentration dependence of the emission yield at the higher DNA concentrations, we measured the time-resolved luminescence decay of intercalated Δ-$Os(phen)_2dppz^{2+}$ by TCSPC, also as a function of DNA loading. Luminescence decay traces corresponding to $R_{nuc:Os}$ = 5, 10, 20, 100 appear as an inset in Figure 4. Emission from Δ-$Os(phen)_2dppz^{2+}$, like the ruthenium analogue, is best described with a biexponential fit, and the results of nonlinear

(23) Juris, A.; Balzani, V.; Barigelletti, F.; Campagna, S.; Belser, p.; Von Zelewsky, A. *Coord. Chem. Rev.* **1988**, *84*, 85.

(24) Hiort, C.; Lincoln, P.; Nordén, B. *J. Am. Chem. Soc.* **1993**, *115*, 3448.

Table 1. Luminescence Lifetimes for Δ-Os(phen)$_2$dppz^{2+} Bound to DNA

$R_{nuc:Os}$	τ_1 (ns)[a,b]	τ_2 (ns)[a,b]
5	2.3 (43)	13 (56)
10	2.0 (48)	12 (51)
20	1.8 (55)	11 (46)
100	1.5 (76)	9.2 (24)

[a] Excited-state lifetimes were measured for osmium samples (50 μM) in the presence of calf thymus DNA in aerated buffer containing 5 mM Tris, 50 mM NaCl, pH 8.5 at ambient temperature. Error in kinetics data is estimated to be ±10%. [b] The percent contribution of each lifetime to the overall decay is given in parentheses.

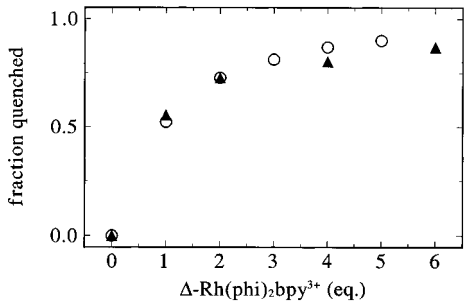

Figure 5. Plot of the fraction of emission quenched ($1 - I/I_0$) for Δ-Os(phen)$_2$dppz^{2+} (▲) and Δ-Ru(phen)$_2$dppz^{2+} (○) bound to DNA as a function of increasing equivalents of Δ-Rh(phi)$_2$bpy^{3+}. For the osmium titration (λ_{exc} = 480 nm; λ_{obs} = 740 nm), quencher was added to 20 μM Os(II), 2 mM nucleotides in 5 mM tris, 50 mM NaCl, pH 8.5, and in the ruthenium titration (λ_{exc} = 480 nm; λ_{obs} = 610 nm), quencher was added to 10 μM Ru(II), 1 mM nucleotides under the same buffer conditions. Equivalent data are observed with 20 μM Ru(II)/2 mM nucleotides.

least squares analysis of the decay traces shown are listed in Table 1. These time-resolved data are in agreement with similar data for Δ-Ru(phen)$_2$dppz^{2+} and indicate identical binding properties for the osmium complex. As is the case for Λ-Ru(phen)$_2$dppz^{2+},[24] the quantum yield for emission from Λ-Os(phen)$_2$dppz^{2+} is significantly lower than that of the Δ-isomer, and therefore we have focused our luminescence and quenching studies on Δ-Os(phen)$_2$dppz^{2+}.

Emission Intensity Quenching. Emission from Os(phen)$_2$dppz^{2+} bound to DNA is quenched by Rh(phi)$_2$bpy^{3+}. In order to examine this quenching in detail, we have titrated the quencher, Δ-Rh(phi)$_2$bpy^{3+}, into solutions of donor, Δ-Os(phen)$_2$dppz^{2+}, bound to sonicated calf-thymus DNA. Importantly, Ru(phen)$_2$dppz^{2+} complexes show appreciable luminescence with synthetic polymers of different sequence, and NMR and binding studies of the ruthenium analogue indicate that these dppz complexes bind to the DNA duplex in an essentially random, sequence-neutral fashion.[11] Similarly, DNA photocleavage studies of Rh(phi)$_2$bpy^{3+} in the absence[12] and presence[15] of Ru(phen)$_2$dppz^{2+} or Ru(bpy)$_2$dppz^{2+} indicate that the rhodium complex binds DNA with sequence neutrality at these concentrations and there is no perturbation in this binding profile by the ruthenium complexes; hence we find no evidence for binding cooperativity.[25] Thus, in an effort to maintain large donor−acceptor separations given the random occupation of both donor and acceptor on the helix, the $R_{nuc:Os}$ ratio was held constant at 100:1.

The results of such a titration, plotted as the fraction of emission intensity quenched (fraction quenched) as a function of acceptor concentration, are shown in Figure 5. With just 1 equiv of quencher, where the average donor−acceptor separation is 25 base pairs (88 Å), the emission is quenched by almost 50%. The fraction quenched reaches saturation at 0.9 with 6 equiv of rhodium. Also plotted in Figure 5 are the results of the same experiment with Δ-Ru(phen)$_2$dppz^{2+} as donor.[15] Over the concentration ranges examined, the osmium and ruthenium quenching profiles are strikingly similar. These results therefore indicate a similar efficiency for the quenching of each donor.

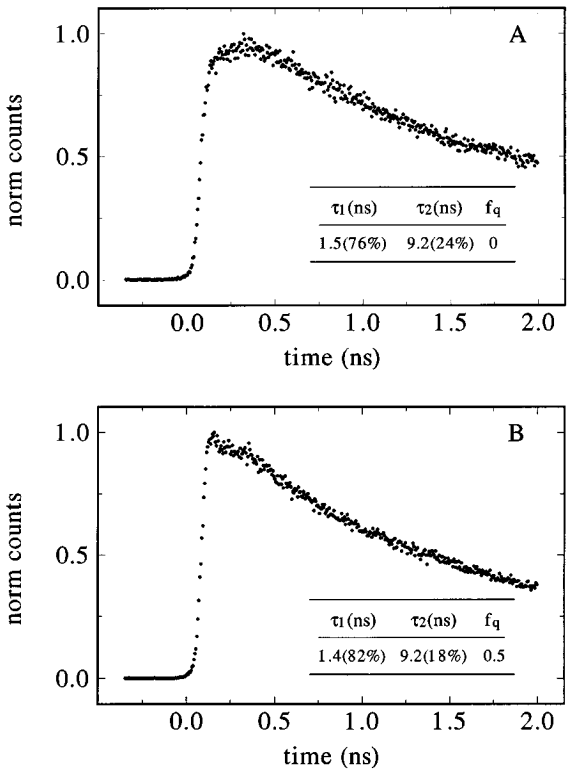

Figure 6. Time-resolved luminescence decay of Δ-Os(phen)$_2$dppz^{2+} bound to DNA in the absence (A) and presence (B) of 1 equiv of Δ-Rh(phi)$_2$bpy^{3+}. Shown are normalized counts. The lifetimes of the decays and the fraction of emission quenched (f_q) are indicated below each trace. The observed quenching is primarily manifested as a decrease in the intensity at zero time, since the minor changes in decay kinetics for the quenched sample do not account for the 50% quenching. Conditions: 50 μM Os, 5 mM nucleotides in 5 mM tris, 50 mM NaCl, pH 8.5; λ_{exc} = 590 nm, λ_{obs} = 775 nm.

We have used TCSPC with ∼150 ps resolution to examine the rate of this Os(phen)$_2$dppz^{2+} quenching. We find that the majority of the quenching is static relative to the resolution of this instrument and thus primarily appears as a decrease in the intensity at time zero. Importantly, the amount of quenching due to this decrease in the intensity at time zero increases with increasing quencher concentration, and no substantial change in decay kinetics occurs as a function of quencher. Figure 6 compares the luminescence decay profile of Δ-Os(phen)$_2$dppz^{2+} in the presence and absence of 1 equiv of Δ-Rh(phi)$_2$bpy^{3+}. A small amount of response-limited signal is observed for quenched Δ-Os(phen)$_2$dppz^{2+}, but the overall kinetic profile is nearly unchanged. This response-limited signal may actually be derived from rhodium-based emission. Therefore, these measurements provide a lower limit of 7×10^9 s^{-1} for the rate constant describing the ultrafast quenching reaction.

Electron Transfer Intermediates. Scheme 1 illustrates the cycle for electron transfer reactions between Os(phen)$_2$dppz^{2+} and Rh(phi)$_2$bpy^{3+} bound to DNA. In order to attribute the emission intensity quenching described above to photoinduced electron transfer (k_{et}), we have used transient absorption spectroscopy to identify and characterize the intermediate consistent with such a DNA-mediated electron transfer reaction.

(25) Arkin, M. R.; Stemp, E. D. A; Turro, C.; Turro, N. J.; Barton, J. K. *J. Am. Chem. Soc.* **1996**, *118*, 2267.

Scheme 1

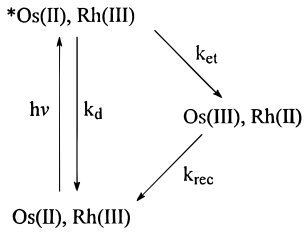

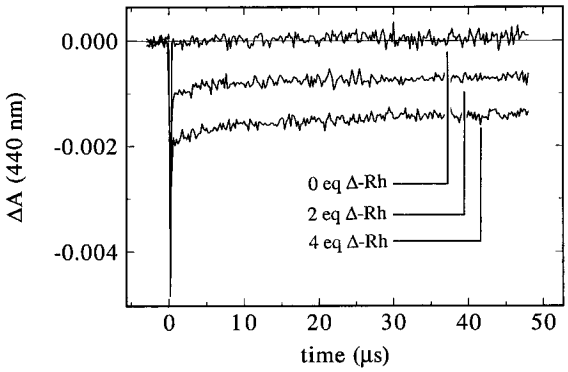

Figure 7. Transient signals observed at 440 nm upon excitation (480 nm) of $Os(phen)_2dppz^{2+}$ bound to DNA in the presence of 0, 2, and 4 equiv Δ-$Rh(phi)_2bpy^{3+}$. As the rhodium concentration is increased, a long-lived signal is observed. The kinetics of these transients are multiphasic with lifetimes on the order of 5 μs and longer. Conditions: 20 μM Os, 2 mM nucleotides in 5 mM tris, 50 mM NaCl, pH 8.5.

Figure 7 shows the transient signals observed upon 440 nm excitation of $Os(phen)_2dppz^{2+}$ at 480 nm in the presence of 0, 2, and 4 equiv of Δ-$Rh(phi)_2bpy^{3+}$. As expected for $Os(phen)_2dppz^{2+}$ in the absence of acceptor, the MLCT excited state is seen as a bleach at 440 nm which returns to baseline within the instrument response, consistent with the short excited-state lifetime of the DNA-bound complex. On the other hand, in the presence of Δ-$Rh(phi)_2bpy^{3+}$, a long-lived signal which persists well into the microsecond regime grows in with increasing acceptor concentration. Owing to the correlation between transient signal intensity and acceptor concentration, such a signal likely reflects an electron transfer intermediate. By analogy to photoinduced electron transfer studies with other polypyridyl complexes,[18,26] we expected this intermediate to correspond to the oxidized donor.

In an effort to assign unambiguously the observed long-lived transient to the Os(III) oxidized donor, the signal height as a function of wavelength was measured and compared to known Os(III)−Os(II) difference spectra. A static Os(III)−Os(II) difference spectrum was obtained by chemical oxidation of $Os(phen)_2dppz^{2+}$ to $Os(phen)_2dppz^{3+}$ with Ce(IV).[18] Additionally, transient absorption spectroscopy was used to observe Os(III) generated by oxidizing photoexcited $Os(phen)_2dppz^{2+}$ bound to DNA with the well-characterized electron acceptor $Ru(NH_3)_6^{3+}$; the wavelength dependence of the signal obtained using this flash-quench methodology provides an Os(III)−Os(II) kinetic difference spectrum.

Figure 8A shows the spectral changes that accompany the oxidation of $Os(phen)_2dppz^{2+}$ to $Os(phen)_2dppz^{3+}$ by Ce(IV) in water. For the Os(II) species, the visible absorption is dominated by the formally singlet MLCT transitions (λ_{max} = 430 nm and 472) and the triplet MLCT transitions which tail out beyond 720 nm. The $\pi-\pi^*$ IL transition centered on the

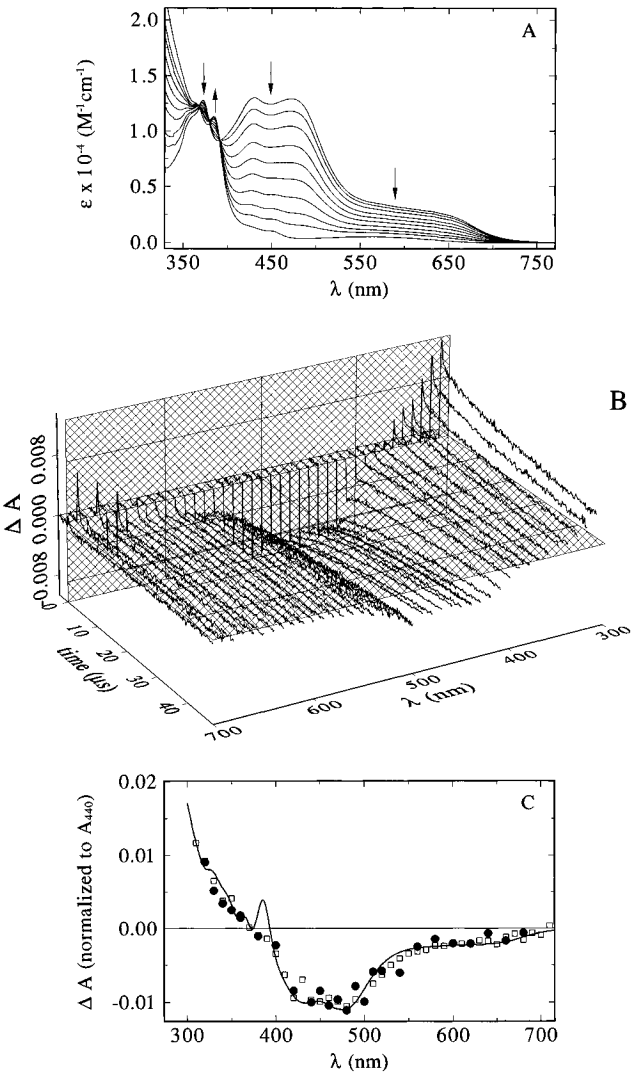

Figure 8. Spectral characterization of the chemical and photochemical oxidation of $Os(phen)_2dppz^{2+}$. (A) Spectral changes which accompany the oxidation of aqueous $Os(phen)_2dppz^{2+}$ (~0.1 mM) to $Os(phen)_2dppz^{3+}$ with the addition of dilute $Ce(NO_3)_6^{2-}$. (B) Transient absorption signals obtained by oxidation of photoexcited $Os(phen)_2dppz^{2+}$ (15 μM) bound to DNA (1.5 mM nucleotides in 5 mM tris, 50 mM NaCl, pH 8.5) by $Ru(NH_3)_6^{3+}$ (300 μM). The full time course of the transient signal intensity is also plotted as a function of wavelength to show the time dependence of the resulting spectrum. (C) Static Os(III)−Os(II) difference spectrum (solid line) generated by subtracting the Os(II) absorption spectrum from that of the fully oxidized complex. Also shown are the Os(III)−Os(II) kinetic difference spectrum (□) taken from the signal height of the long-lived transient in Figure 7B, and the wavelength dependence of the rhodium-induced transient (●) observed with quenching of intercalated $Os(phen)_2dppz^{2+}$ (Figure 6). For ease of presentation, the spectra plotted here are normalized at 440 nm owing to substantial hypochromism from 300 to 500 nm for the complex bound to DNA.

phenazine portion of the dppz ligand occurs with λ_{max} = 372 nm. In the oxidized spectrum, the intense charge-transfer transitions are no longer present and a weak transition (ϵ < 1000 M^{-1} cm^{-1}), probably ligand-to-metal charge-transfer (LMCT) in character, occurs around 600 nm.[27]

Transient signals obtained by oxidation of photoexcited $Os(phen)_2dppz^{2+}$ bound to DNA by $Ru(NH_3)_6^{3+}$ are plotted in Figure 8B. In order to show the time course of the signal as well as its wavelength dependence, the changes in absorbance are plotted in a three-dimensional representation. To obtain a

(26) Indelli, M. T.; Bignozzi, C. A.; Harriman, A.; Schoonover, J. R.; Scandola, F. *J. Am. Chem. Soc.* **1994**, *116*, 3768.

(27) Bryant, G. M.; Fergusson, J. E. *Aust. J. Chem.* **1971**, *24*, 275.

Table 2. Electrochemical Potentials[a] for Osmium and Ruthenium Complexes

complex	E^0 (*2+/3+)[b]	E^0 (3+/2+)[c]	reductions[c] 1	2	3
$Os(phen)_2dppz^{2+}$	0.78	1.15	−0.61	−0.98	−1.21
$Os(phen)_3^{2+}$		1.11	−0.92	−1.06	
$Ru(phen)_2dppz^{2+}$ [d]	0.60	1.60			
$Ru(bpy)_2dppz^{2+}$ [e]		1.48	−0.62	−1.06	−1.27

[a] In dry DMF with 0.1 M tetrabutylammonium hexafluorophosphate; scan rate = 0.1 V/s. [b] Excited-state oxidation potential reported in eV. [c] Reported in V vs NHE. [d] Reference 10a. [e] Reference 28, converted to NHE.

typical Os(III)−Os(II) kinetic difference spectrum, we simply extract a time slice ($t > \tau_{MLCT}$) from this plot.

In Figure 8C we show (as a solid line) the static Os(III)−Os(II) difference spectrum constructed by subtracting the $Os(phen)_2dppz^{2+}$ absorption spectrum from that of the oxidized complex. Also in Figure 8C, plotted as an overlay above the static difference spectrum, is the wavelength dependence of the absorbance changes observed for the oxidation of photoexcited $Os(phen)_2dppz^{2+}$ bound to DNA. As expected, both the static and kinetic Os(III)−Os(II) difference spectra are in good agreement. Noteworthy in the kinetic spectrum, however, is the deviation at ∼375 nm which is attributed to the hypochromism of the dppz IL band where the complex is bound to DNA.

We also present the spectrum of the transient observed for the quenching of $Os(phen)_2dppz^{2+}$ by Δ-$Rh(phi)_2bpy^{3+}$ in Figure 8C. Indeed, throughout the wavelength range investigated, this signal is in excellent agreement with the known Os(III)−Os(II) difference spectra. Thus, as anticipated, we attribute theobserved transient to an Os(III) electron transfer intermediate. Like the kinetic difference spectrum obtained by oxidizing photoexcited $Os(phen)_2dppz^{2+}$ bound to DNA, the difference spectrum for this Os(III) intermediate deviates slightly from the static Os(III)−Os(II) difference spectrum. This deviation is again derived from the hypochromism in the dppz IL band and, importantly, shows that the complex remains bound throughout the reaction. This spectral feature indicates that neither the transient observed nor the quenching observed arises from a trivial displacement of the complex from the helix, consistent with the $k_{off} < 100\ s^{-1}$ determined by NMR[11] for the isostructural ruthenium analogue. The observation of such an electron transfer intermediate establishes photoinduced electron transfer as the operative mechanism in the fast quenching of emission from intercalated $Os(phen)_2dppz^{2+}$ by Δ-$Rh(phi)_2bpy^{3+}$.

Cyclic Voltammetry. CV was used to characterize the oxidation and reduction potentials of $Os(phen)_2dppz^{2+}$. These results along with similar data for $Ru(phen)_2dppz^{2+}$ are listed in Table 2.[10a,18,28] A reversible oxidation wave corresponding to the 3+/2+ couple is observed at 1.1 V (vs NHE). By analogy to the reduction of $Ru(bpy)_2dppz^{2+}$ and $Os(phen)_3^{2+}$ measured by CV, the reduction at −0.62 V is assigned to a one-electron reduction centered on the dppz ligand, while the remaining two correspond to one-electron reductions on the phenanthrolines. As expected,[18] oxidation of $Os(phen)_2dppz^{2+}$ is ∼500 mV more favorable compared to the ruthenium complex. Additionally, based on an E_{00} value of 1.9 eV for $Os(phen)_2dppz^{2+}$,[29] the excited state of the osmium complex is ∼200 mV more reducing compared to that of $Ru(phen)_2dppz^{2+}$. The reduction potentials of $Os(phen)_2dppz^{2+}$, however, are not significantly different from those of the ruthenium analogue. These observations are consistent with CV data for other polypyridyl complexes of ruthenium and osmium[18] and indicate a similar absolute energy for the HOMO in the MLCT excited state of $M(phen)_2dppz^{2+}$ (M = Os(II), Ru(II)) complexes.

Discussion

DNA Binding Properties. A common way to expand the scope of redox reactions between polypyridyl metal complexes is to modify the ligand properties of the reactants. However, in DNA-mediated electron transfer reactions, we find that the DNA binding properties of the reactants play a significant role in determining the efficiency of the reaction, and these binding profiles are sensitive to small perturbations in the ligand structures which make up the complex.[11,15,25] Thus, in order to change the properties of our electron donor without altering its DNA binding properties, we have substituted osmium for ruthenium in complexes of the type $M(phen)_2dppz^{2+}$. Even though the lanthanide contraction leads to a small difference in the ruthenium and osmium ionic radii,[30] this small difference is insignificant compared to the full dimensions of the coordination complex. Hence, substitution of osmium for ruthenium should not perturb the binding profile of the metal complex given the same ligand sphere.

We have shown $Os(phen)_2dppz^{2+}$ to bind to DNA by intercalation of the dppz ligand. Evidence for intercalation is provided by the strong hypochromism in the IL $\pi-\pi^*$ transition centered on the dppz ligand observed by visible spectroscopy. This intercalation of the dppz ligand gives rise to the molecular light switch properties of the complex[17] since emission in aqueous solutions is observed only when the dppz nitrogens are protected from solvent, as provided by intercalation. Therefore, since only complexes bound to the polymer emit, we have been able to examine the binding profile of $Os(phen)_2dppz^{2+}$ by studying the luminescence as a function of DNA concentration by both steady-state and time-resolved techniques.

At intermediate and high $R_{nuc:Os}$ values, we find that, in the presence of DNA, Δ-$Os(phen)_2dppz^{2+}$ emission decays as a biexponential, with lifetimes in the range of 1.5−2.0 ns and and 9.2−13 ns (Table 2). Such a biphasic emission profile, observed previously for $Ru(phen)_2dppz^{2+}$, has been attributed to two intercalative binding geometries which provide differential protection of the phenazine nitrogens.[11] Within this model, which has been supported by two-dimensional ^1H NMR studies,[11] the shorter lived species corresponds to an intercalative binding geometry with the dppz ligand oriented along the base-pair axis in a side-on fashion, and the longer lifetime reflects an intercalative geometry where the ligand is intercalated perpendicular to the base-pair axis in a head-on mode. The percent contribution of each lifetime to the overall luminescence decay reflects the relative distribution of side-on and head-on binding populations. As indicated in Table 2, at intermediate loadings, the two geometries are present in almost a 1:1 ratio. As the concentration of DNA is increased, the shorter lived species begins to dominate the decay.

As shown in Figure 4, the steady-state emission intensity for Δ-$Os(phen)_2dppz^{2+}$ increases with increasing DNA concentration for $R_{nuc:Os}$ values ranging from 0 to ∼5, with a sharp increase from 5 to 6.25, where the emission yield is maximized. At $R_{nuc:Os}$ values greater than 6.25, the emission yield is seen to decrease with increasing DNA concentration over a broad

(28) Amoual, E.; Homsi, A.; Chambron, J.-C.; Sauvage, J.-P *J. Chem. Soc., Dalton. Trans.* **1990**, 1841.

(29) The E_{00} was estimated as the highest energy point along the emission spectrum (∼640 nm); see ref 23.

(30) Cotton, F. A.; Wilkinson, G. *Advanced Inorganic Chemistry*, 5th ed.; John Wiley & Sons: New York, 1988.

range of $R_{nuc:Os}$ values. The increase in emission yield with increasing DNA concentration reflects the binding of more complexes to the polymer, since only those complexes bound to DNA show detectable emission. The large enhancement in emission yield going from $R_{nuc:Os} = 5$ to 6.25 likely reflects self-quenching of the emission in the early region of the titration where the complexes are highly loaded onto the DNA.[31] It is noteworthy that quenching experiments performed here with rhodium acceptors are accomplished at substantially higher DNA:metal ratios.

The observed decrease in emission yield for $R_{nuc:Os} > 6.25$ is manifested by a change in luminescence decay profile (Table 2). For large $R_{nuc:Os}$ values, the side-on binding mode, which exhibits a shorter excited-state lifetime, contributes most to the overall decay, leading to a decrease in steady-state emission intensity. The DNA concentration dependence in the relative distribution of side-on and head-on binding populations may reflect spatial constraints on binding geometry when the helix is heavily loaded with complexes. In addition to the changes in binding orientation, the excited-state lifetimes for each binding geometry also decrease slightly with increasing DNA concentration. Such a decrease may also reflect a concomitant decrease in helical rigidity as the metal complexes become more dilute along the polymer, giving rise to a greater propensity for vibrational deactivation of the excited state.

The kinetic analysis of luminescence data which describes the $Os(phen)_2dppz^{2+}$ binding characteristics is essentially identical to that used for $Ru(phen)_2dppz^{2+}$ previously.[11,24] Thus, $Os(phen)_2dppz^{2+}$ provides an isostructural analogue for $Ru(phen)_2dppz^{2+}$ while at the same time exhibiting a broader absorption profile, red-shifted emission with excited-state decay kinetics on a shorter time scale ($\tau < 10$ ns), and access to a 3+ oxidation state which is stabilized by ~500 mV compared to the ruthenium species.

Donor Properties and Quenching Efficiency. As evident in the quenching titrations, emission from intercalated Δ-$Os(phen)_2dppz^{2+}$ is significantly quenched by Δ-$Rh(phi)_2bpy^{3+}$, which also binds to DNA by intercalation. The decay kinetics for Δ-$Os(phen)_2dppz^{2+}$ in the presence and absence of Δ-$Rh(phi)_2bpy^{3+}$ show little difference, as the quenching is revealed as a loss in intensity at zero time. TCSPC with ~150 ps resolution allows us to set a lower limit of 7×10^9 s^{-1} for the quenching constant.

The quenching of Δ-$Os(phen)_2dppz^{2+}$ as a function of acceptor concentration furthermore matches that of Δ-$Ru(phen)_2dppz^{2+}$ quite closely. Since the spectral characteristics for the two complexes differ significantly, the quenching cannot depend strongly on spectral overlap of donor emission with acceptor absorption. In fact, spectral overlap of osmium emission and rhodium absorption is vanishingly small. Hence, *this correlation rules out any significant contribution by energy transfer to the quenching of either* $Os(phen)_2dppz^{2+}$ *or* $Ru(phen)_2dppz^{2+}$ *by* $Rh(phi)_2L^{3+}$ *(L = bpy, phen).*

Loading Dependence of Quenching Efficiency. While quenching reactions between donors and acceptors bound noncovalently and randomly to DNA are not intended to provide a quantitative evaluation of the distance dependence of DNA-mediated electron transfer, we may, nonetheless, point to novel aspects of these quenching titrations as a function of loading on the helix. At 1 equiv of acceptor, we observe ~50% quenching of the osmium lumiphore, but only 2% of donor−acceptor separations are expected at closest contact with random binding of the metallointercalators on the helix. Importantly, while quenching must be possible at longer distances, it can also not occur over infinite distance, since this latter case would require complete quenching of donor luminescence by 1 equiv of acceptor. Hence our observation of 50% quenching under these conditions demonstrates that the quenching reaction does indeed exhibit a loading dependence and these quenching titrations are qualitatively consistent with the occurrence of electron transfer events at separations of up to 20 base pairs.[32]

Effect of Donor Excited-State Lifetime. Given the 2 orders of magnitude difference in excited-state lifetimes for Δ-$Os(phen)_2dppz^{2+}$ bound to DNA versus Δ-$Ru(phen)_2dppz^{2+}$ bound to DNA, the similarity in $M(phen)_2dppz^{2+}$ quenching profiles demonstrates a lack of sensitivity in quenching efficiency to the excited-state lifetimes of the osmium and ruthenium donors. The absence of such a dependence suggests that diffusion plays only a minor role, if any, in the quenching, a result consistent with the notion that the electron transfer is a first-order process, proceeding through the DNA double helix. This observation is in contrast to experiments with tris(phenanthroline) metal complexes as reactants which bind DNA both by intercalation and by groove binding.[9] Interestingly, we observe that the static quenching of Δ-$Ru(phen)_2dppz^{2+}$ by Δ-$Rh(phi)_2bpy^{3+}$ is accompanied by a minor (<10%) component of slower quenching occurring on a time scale of ≥100 ns. Since the excited-state lifetime of Δ-$Os(phen)_2dppz^{2+}$ bound to DNA is less than 10 ns, similarly slow processes could not contribute to quenching of the osmium complex.

Considerations of Energetics. Substitution of osmium for ruthenium in $M(phen)_2dppz^{2+}$ complexes allows for evaluation of the role energetic parameters such as the 3+/2+ redox couple and the excited-state oxidation potential of the donor play in determining electron transfer quenching efficiency. As illustrated in Table 2, $Os(phen)_2dppz^{3+}$ is stabilized by ~500 mV over $Ru(phen)_2dppz^{3+}$, and the excited state of the osmium complex is ~200 mV more reducing compared to the ruthenium analogue. As described above, the greater potential for reduction by the osmium excited state may give rise to a slight increase in quenching efficiency, but to first order, the efficiency of quenching photoexcited $M(phen)_2dppz^{2+}$ complexes bound to DNA by intercalated $Rh(phi)_2bpy^{3+}$ is largely insensitive to both the 3+/2+ redox couple and the excited-state oxidation potential. Importantly, since we have not resolved the individual rates of forward electron transfer for the osmium and ruthenium donors, the comparison holds here only for the efficiency of the quenching reaction.[15]

As an explanation for such an observation, we consider the absolute energies of the $M(phen)_2dppz^{2+}$ excited-state HOMOs. Reduction of the phenazine portion of the dppz ligand occurs at essentially the same potential in $Os(phen)_2dppz^{2+}$ and $Ru(phen)_2dppz^{2+}$. Furthermore, the difference between E_{00}(Ru) and E_{00}(Os) is represented by the difference in the 3+/2+ reduction potentials for the two complexes. Thus, on the basis of these data and the MLCT character of the $M(phen)_2dppz^{2+}$ excited states, the excited-state HOMOs are judged to be equivalent in absolute energy.[33] Therefore, if the efficiency of photoinduced electron transfer from $M(phen)_2dppz^{2+}$ were

(31) Note that this titration differs from others[24] in that DNA is titrated into lumiphore solution, which results in high loadings of metal on the DNA in the early portions of the titration; high loadings promote self-quenching. Self-quenching of emission has also been observed for $Ru(TMP)_3^{2+}$ (TMP = 4,5,6,7-tetramethyl-1,10-phenanthroline) complexes bound cooperatively to DNA without intercalation. See: Mei, H.-Y.; Barton, J. K. *J. Am. Chem. Soc.* **1986**, *108*, 7414.

(32) Application of a sphere of action model to earlier quenching titrations[10a] of *rac*-$Ru(phen)_2dppz^{2+}$ bound to DNA with *rac*-$Rh(phi)_2phen^{3+}$ yielded ~10 base pairs as the critical distance required for reaction. For the quenching titrations described here using enantiomers bound to DNA, deviations from such a model are found, with quenching apparently more favored at lower loadings.

limited by electronic access to a high-energy DNA bridge originating from the donor excited state,[1,2] the efficiency of quenching would be expected to be similar for osmium and ruthenium. An alternative explanation for the observed leveling effect with respect to free energy for these photoinduced reactions lies in the possibility that electron transfer proceeds from the donor excited state into an acceptor excited state.[34]

Intermediates. Just as the lack of spectral overlap between the osmium emission and rhodium absorption points to photoinduced electron transfer rather than energy transfer, the observation of an intermediate establishes firmly electron transfer as the quenching mechanism. Transient absorption spectroscopy allowed us to detect a long-lived signal which grows in with increasing quencher concentration. Using Ce(IV) to oxidize $Os(phen)_2dppz^{2+}$ free in solution and $Ru(NH_3)_6^{3+}$ to oxidize photoexcited $Os(phen)_2dppz^{2+}$ bound to DNA, we have generated Os(III)−Os(II) difference spectra. Comparison of the difference spectrum of the long-lived transient observed for the quenching of $Os(phen)_2dppz^{2+}$ by $Rh(phi)_2bpy^{3+}$ bound to DNA to the known Os(III)−Os(II) difference spectra verifies that the signal observed corresponds to the oxidized donor, $Os(phen)_2dppz^{3+}$. Similar spectral evidence for an electron transfer intermediate produced in the DNA-mediated electron transfer quenching of $Ru(DMP)_2dppz^{2+}$ by $Rh(phi)_2bpy^{3+}$ has been reported;[16] however, such a full spectral characterization could not be achieved.

While providing a description of the oxidized donor, the difference spectrum of the rhodium-induced intermediate yields little information concerning the reduced acceptor ($Rh^{II}(phi)_2$-bpy or $Rh^{III}(phi)(phi)^{-}bpy$). Indeed, according to Scheme 1, the spectrum of the electron transfer intermediate should contain some contribution from the reduced acceptor. However, the closeness of the intermediate spectrum to the known Os(III)−Os(II) difference spectrum indicates that the change in extinction coefficient upon reduction of the acceptor bound to DNA must be small relative to that for oxidation of the donor.[35]

In addition to formation of Os(III) via photoinduced electron transfer from the Os(II) excited state to ground-state Rh(III), the same intermediate would also be formed by hole transfer if a Rh(III) excited state were to oxidize ground-state Os(II). While such a mechanism has been observed recently in a Ru(II)/Rh(III) dyad,[26] we have been able to rule out hole transfer here by shifting the excitation to wavelengths where the Rh(III) complex does not absorb. Indeed, the fraction of $Os(phen)_2dppz^{2+}$ emission quenched by Δ-$Rh(phi)_2bpy^{3+}$ is not changed whether excitation occurs at 480, 532, or 580 nm, indicating that the Rh(III) excited state does not quench the Os(II) emission. Furthermore, we observe the same long-lived electron transfer intermediate with each of the above excitation wavelengths, and therefore, production of Os(III) must occur by electron transfer rather than hole transfer. Moreover, we can eliminate any questions of multiphoton chemistry in the production of Os(III) since observation of this intermediate is not systematically affected by variations in power or excitation wavelength.

The detection of the long-lived intermediate, in conjunction with ultrafast emission and transient absorption measurements,[15] allows us to assign electron transfer as the mechanism of quenching. Since the long-lived intermediate corresponds to only a small fraction of the electron transfer products, the observation of the transient on the microsecond time scale does not in itself prove an electron transfer mechanism for *all* of the luminescence quenching. Using ultrafast TCSPC, we have shown that the quenching constant is $>3 \times 10^{10}$ s^{-1} for both $*Ru(phen)_2dppz^{2+}$ and $*Os(phen)_2dppz^{2+}$, while transient absorption measurements show that, for quenched donors, most of the ground-state recovery occurs with a rate of $\sim 1 \times 10^{10}$ s^{-1}.[37] Because no 10^{10} s^{-1} component is present in the emission dynamics, the kinetics measured by picosecond transient absorption must represent the recombination reaction. The fact that not all of the back electron transfer occurs on the picosecond time scale is reflected in the detection of a long-lived intermediate. Taken together, these results clearly show that electron transfer is the quenching mechanism on all time scales. The experiments described here allow us to characterize spectroscopically the intermediate.

Long-lived species corresponding to the oxidized electron donors have now been observed for $Os(phen)_2dppz^{2+}$ and $Ru(DMP)_2dppz^{2+}$, but in the case of $Ru(phen)_2dppz^{2+}$, no such intermediate can be detected. The distinction between $Os(phen)_2$-$dppz^{2+}$ and $Ru(phen)_2dppz^{2+}$ in terms of long-lived intermediates is noteworthy given the similarity in their quenching profiles. To account for these differences, we again consider the relative energetics, or stabilities, of the osmium and ruthenium species. On the basis of the larger (∼500 mV) reduction potential for $Ru(phen)_2dppz^{3+}$ compared to that for $Os(phen)_2dppz^{3+}$ (Table 2), the $Ru(phen)_2dppz^{3+}$ intermediate is more reactive. One possible fate of a long-lived Ru(III) species may be reaction with the DNA by oxidation of a guanine base.[8,31] Such a reaction would be less favorable, likely prohibitively so, in the case of osmium, as has recently been observed for intercalated $Os(bpy)_2dppz^{3+}$ generated by cyclic voltammetry.[38,39]

It is also instructive to compare the long-lived intermediates observed for $Os(phen)_2dppz^{2+}$ and $Ru(DMP)_2dppz^{2+}$. For the

(33) Such an orbital arrangement is consistent with the large differences between E_{MLCT}(Os) and E_{MLCT}(Ru) being manifested by the difference in energy between the $5d^6$ and $4d^6$ ground-state configurations for osmium(II) and ruthenium(II), respectively.

(34) When the formation of reduced acceptor in the excited state via photoinduced electron transfer is thermodynamically favorable, such a reaction may be faster than electron transfer to ground-state acceptor if the latter reaction is in the inverted region. Indeed, the inverted effect, in which rates decrease with increasing driving force (Marcus, R. A. *J. Chem. Phys.* **1965**, *43*, 2654), has been observed only in recombination reactions. In our case, the *Rh(II) excited-state energy is likely to be 1.8−2.0 V; thus electron transfer could still be favorable from both $*Ru(phen)_2dppz^{2+}$ and $*Os(phen)_2dppz^{2+}$. For photoinduced electron transfer to ground-state rhodium to fall in the inverted region, the reorganization energy must be low (λ < 0.6 V), a reasonable possibility for a reaction in which DNA bases act as solvent. See: Mines, G. A.; Bjerrum, M. J.; Hill, M. G.; Casimiro, D. R.; Chang, I.-J.; Winkler, J. R.; Gray, H. B. *J. Am. Chem. Soc.* **1996**, *118*, 1961. McCleskey, T. M.; Winkler, J. R.; Gray, H. B. *Inorg. Chim. Acta* **1994**, *225*, 319. McCleskey, T. M.; Winkler, J. R.; Gray, H. B. *J. Am. Chem. Soc.* **1992**, *114*, 6935.

(35) Transient absorption experiments indicate that $\Delta\epsilon \leq 3000$ M^{-1} cm^{-1} for the reduction of $Rh(phi)_2L^{3+}$ (L = phen, bpy) free in solution (Turro, C.; Evenzahav, A.; Bossman, S. H.; Barton, J. K.; Turro, N. J. *Inorg. Chim. Acta*, in press). On the basis of our lack of observation of the reduced acceptor in these DNA-mediated electron transfer reactions, this change in extinction coefficient must be attenuated for the complex bound to DNA. In addition, some decomposition is possible, since the phi ligand or its radical anion is expected to be unstable if dissociated from the metal center.

(36) The oxidation potential of guanine has been estimated to be between ∼1.1 and ∼1.5 V *vs* NHE: Kittler, L.; Löber, G.; Gollmick, F. A.; Berg, H. *J. Electroanal. Chem.* **1980**, *116*, 503. Jovanovic, S. V.; Simic, M. G. *Biochim. Biophys. Acta* **1989**, *1008*, 39.

(37) For example, $k_{rec} = 1.1 \times 10^{10}$ s^{-1} and 9×10^9 s^{-1} for $Os(phen)_2$-$dppz^{3+}$ and $Ru(phen)_2dppz^{3+}$, respectively.[15] These recombination rates may support a free energy dependence which is consistent with previous notions that this reaction occurs in the Marcus inverted region. However, such a small difference in rate may be more consistent with electron transfer into an excited-state manifold of the acceptor, which then reduces the Os(III) before relaxing to the ground state. In this case, the actual driving force would be different from the apparent free energy of reaction.[34]

(38) Welch, T. W.; Corbett, A. H.; Thorp, H. H. *J. Phys. Chem.* **1995**, *99*, 11757.

Os(III) intermediate, the long-lived signal observed grows in qualitatively but not quantitatively with quencher concentration. For the ruthenium species, the intermediate signal height parallels the fraction quenched. In contrast, the signal height for the Os(III) intermediate is seen to double going from 2 to 4 equiv of acceptor while the amount of quenching increases modestly from 73% to 80%. Additionally, the yield (<10%) of the long-lived Os(III) species is less than the yield (10−30%) of long-lived $Ru(DMP)_2dppz^{3+}$. We can account for this difference in yields since, for $Os(phen)_2dppz^{2+}$, more back electron transfer is occurring with k_{rec} in the 10^{10} s^{-1} regime than for $Ru(DMP)_2dppz^{2+}$.[15] We do not yet understand the basis for this wide range of back-electron-transfer rates. The fast recombination may result in part from electron transfer from the rhodium excited-state manifold (*vide supra*) with slower reaction occurring from the rhodium ground state. Additionally, such a distribution may be the consequence of a decoupling of donor and acceptor by defects in base stacking, which arise from the structural polymorphism of DNA and have an increasing probability of occurring with an increase in donor−acceptor separation.

Implications for Long-Range Electron Transfer. Metallointercalators allow us to probe systematically how the DNA π-stack might mediate electron transfer. Here, we have described the electron transfer reactions between $Os(phen)_2dppz^{2+}$, an isostructural analogue for $Ru(phen)_2dppz^{2+}$, and $Rh(phi)_2bpy^{3+}$ bound to DNA. For these donors we have observed substantial quenching despite low reactant loadings on the helix. Moreover, we demonstrate here for osmium that the quenching is remarkably fast ($k_{et} > 7 \times 10^9$ s^{-1}).

These results point either to fast quenching processes occurring over large separations of donor from acceptor on the helix or to the cooperative clustering of donor with acceptor on the helix. Spectroscopic and photocleavage studies have been consistent with random binding of donors and acceptors and show no evidence for a cooperative interaction between the intercalators.[11,12,15] Moreover quenching studies in anionic micelles,[25] where clustering might be expected to be encouraged, also have shown no evidence for cooperativity and instead reveal dynamic quenching on the nanosecond time scale. Furthermore, the titrations described here for osmium and elsewhere for ruthenium[10a] are consistent with results obtained on the mixed-metal oligomeric assembly in which ruthenium and rhodium intercalators were covalently attached and stacked at opposite ends of a 15-mer duplex where quenching was observed on a subnanosecond time scale.[10b]

Here osmium analogues have been valuable in elucidating and eliminating mechanistic explanations for this quenching. Importantly, we have established that electron transfer is the mechanism for this fast quenching, and, given the similarity in quenching profiles for osmium and ruthenium, energy transfer in the case of both ruthenium and osmium must be ruled out. Lastly, these studies with osmium illustrate the utility of applying coordination chemistry to the study of DNA-mediated electron transfer. Since the electron transfer reactions depend so sensitively upon coupling of the reactants into the DNA bridge, an isostructural metallointercalator which exhibits distinctive spectroscopic and redox characteristics becomes a valuable tool in dissecting the parameters which determine electron transfer through the DNA helix.

Acknowledgment. We are grateful to the NIH (GM49216 to J.K.B.) for financial support of this work. We also thank the NSF for a predoctoral fellowship to R.E.H. and the American Cancer Society for a postdoctoral fellowship to E.D.A.S. We would also like to thank Dr. J. Winkler and C. N. Kenyon of BILRC for expert technical support and helpful discussions.

JA953941Y

(39) When photoexcited $M(phen)_2dppz^{2+}$ (M = Os, Ru) bound to poly(d(GC)) is oxidized by $Ru(NH_3)_6^{3+}$, a long-lived M(III) intermediate is observed only for M = Os, an observation which suggests that electron transfer from guanine is favorable only for the Ru(III) metallointercalator.